Reply to Referee#2' comments:

Thank you very much for your valuable comments and suggestions. Answers were shown below.

Reviewer #2: General comments:

The manuscript tried to quantify the impact of the unknown HONO source on the concentrations and budgets of HONO, HO_x radicals and RO_2 radicals in the eastern coast of China by utilizing a model simulation and parameterized unknown HONO source strength. To fulfill this meaningful aim, reasonable parameterization of HONO source and uncertainty analysis of the results are important. However, the uncertainty analysis is not found in the manuscript and the parameterization is not fully justified. Hence, this manuscript is recommended to be published in Atmos. Chem. Phys. unless both parameterization justification and uncertainty analysis are well addressed.

Specific comments:

1. parameterization justification:

A. HONO emission is considered. In page 812, line 6-7, you stated that an emission ratio of 2.3% for HONO/NO_2 used in other study is relatively high. However, in page 814, line 15, you choose to use the same ratio of 0.023 in your model. Please explain.

As shown in the Introduction section, Li et al. (2010) used the HONO/NO_2 ratio of 2.3%. The ratio of 2.3% is only applicable for diesel vehicles, so we used the formula ($[0.023 \times f_{DV} + 0.008 \times (1 - f_{DV})] \times f_{TS}$) to calculate HONO emissions. Where f_{DV} denotes the NO_x emission ratio of diesel vehicles to total vehicles, and f_{TS} is the NO_x emission ratio of the traffic source to all anthropogenic sources (Li et al., 2011; An et al., 2013; Tang et al., 2014). The final ratio for HONO/NO_x as HONO emissions was 1.18% in the BTH.

B. You noticed that HONO chemistry is different near the surface and over the surface within 1000 m. Is this difference explained by the NO_2, $J(NO_2)$ and aerosol surface density? Why NO_2 heterogeneous reactions on ground surface is not considered in your model?

(i) The differences of HONO concentrations near the surface and over the surface within 1000 m can be calculated from the formula $P_{unknown} \approx 19.60\ [NO_2] \cdot J(NO_2)$ when those of NO_2 mixing ratios and $J(NO_2)$ are known. However, the specific chemistry for HONO formation near the surface and over the surface within 1000 m is still unknown because this formula is a statistical result. The specific chemistry for HONO formation near the surface and over the surface within 1000 m is beyond the aim of this paper, and will be investigated in the future.

(ii) Whether NO_2 heterogeneous reactions on ground surface is a source of HONO is still argued. Several model studies (e.g., Li et al., 2010; Wong et al., 2013) have suggested that the NO_2 heterogeneous reactions on ground surface were a possible source of daytime HONO, however, field experiments showed a good correlation between concentrations of particulate matter and HONO (An et al., 2009), or between aerosol surface area and HONO

concentrations (Ziemba et al., 2010), suggesting that aerosol surface is the dominant reaction substrate and that stationary sources (e.g., buildings and soils) are likely insignificant (Ziemba et al., 2010). So more field experiments are needed to validate this mechanism, which could be discussed in the future.

C. In page 811, photo-enhanced heterogeneous reactions and photolysis of surface-adsorbed HNO_3 are summarized as HONO sources. Why these two sources are excluded in your model?

(i) For photolysis of surface-adsorbed HNO_3, only one laboratory study about this reaction was conducted (Zhou et al., 2002b, 2003). A chamber study demonstrated that the photolysis of nitrate which was recently postulated for the observed photolytic HONO formation on snow, ground, and glass surfaces, can be excluded in the chamber (Rohrer et al., 2005). So more laboratory and field studies are required to validate this mechanism, which could be considered in our future work.

(ii) For photo-enhanced heterogeneous reactions, our formula $P_{unknown} \approx 19.60[NO_2] \cdot J(NO_2)$ has some implications.

D. The unknown source strength ($19.60*NO_2*S/V$) is fitted using HONO measurement globally. Is it good for China eastern coast?

We used the data from 13 field measurement campaigns around the globe. The reasons are below:

(i) We want to know whether the correlations of the $P_{unknown}$ with NO_2 mixing ratios and $[NO_2] \cdot J(NO_2)$ are consistent around the globe.

(ii) The measurement campaigns of HONO are still limited around the world， especially in China, but a statistical result needs large samples.

(iii) Fig. R1 shows the correlations of the $P_{unknown}$ with $[NO_2]$ and $[NO_2] \cdot J(NO_2)$ in the coastal areas of China, the other countries, and the globe, respectively. Compared with that around the globe (Fig. R1ef), the correlation coefficient (R^2) between the $P_{unknown}$ and $[NO_2]$ was decreased to 0.38 from 0.75, while the correlation coefficient between the $P_{unknown}$ and $[NO_2] \cdot J(NO_2)$ was decreased to 0.48 from 0.80 (Fig. R1abef). However, the linear regression slope of the latter was 17.37 (Fig. R1b), very close to the 19.60 based on the data around the globe (Fig. R1f).

(iv) The description was added in section 2.2: *"For the coastal regions of China, the correlation between the $P_{unknown}$ and $NO_2 \cdot J(NO_2)$ was 0.48, with a linear regression slope of 17.37 (Fig. S2b in the Supplement), which is within the maximum $P_{unknown}$ uncertainty range of 25% (Table S1)."*

2. uncertainty analysis

A. How the uncertainty in parameterization on HONO source impact the model simulation? What kind of improvement have you made compared to previous model work?

(i) The $P_{unknown}$ in this study was calculated by the daytime HONO budget analysis (Photo Stationary State (PSS) approach) below.

$$\frac{d[HONO]}{dt} = \left(P_{OH+NO} + P_{emission} + P_{transport} + P_{unknown}\right) - \left(L_{HONO+hv} + L_{OH+HONO} + L_{deposition} + L_{transport}\right)$$

(Sörgel et al., 2011; Wong et al., 2012; Spataro et al., 2013)

where $\frac{d[HONO]}{dt}$ is the instantaneous rate of HONO, P_{OH+NO} is HONO production rate from R1, $P_{transport}$ is HONO transport processes including horizontal and vertical transports, $P_{emission}$ is direct emissions of HONO from vehicles, $P_{unknown}$ is the additional unknown daytime HONO source(s). In the sink terms, $L_{HONO+hv}$ is HONO photolysis rate, $L_{HONO+OH}$ is HONO loss rate by HONO+OH, $L_{deposition}$ is HONO deposition rate, and $L_{transport}$ is dilution effects through transport processes. When the photolysis frequency of HONO (J_{HONO}) is greater than 1.0×10^{-3} s^{-1}, the lifetime of HONO is less than 17 minutes. Then the influences of transport and deposition on HONO ($P_{transport}$, $L_{deposition}$ and $L_{transport}$) are weak, can be omitted from the equation above. Therefore, the equation could be expressed:

$$P_{unknown} + P_{OH+NO} + P_{emission} \approx L_{HONO+hv} + L_{OH+HONO}$$

The uncertainties in the observed data were added in the Table R1. In the study of Su et al. (2008, 2011), the uncertainty in the $P_{unknown}$ values calculated by the PSS is 10-25%. Sörgel et al. (2011) suggested the uncertainty in the PSS mainly originated from OH measurements with an accuracy of ±18 %. With the same method (PSS), Wong et al. (2012) also proposed an uncertainty of 10-20% in the $P_{unknown}$ values. To assess the impacts of the uncertainty in the $P_{unknown}$ parameterization on production and loss rates of HONO, two sensitivity cases (Case R_{inc} and Case R_{dec}) were performed. Case R_{inc} includes case R_p with an increase of 25% (the maximum uncertainty range according to the previous studies above) in the slope factor

(19.60); Case R_{dec} is the same as case R_p with a decrease of 25% in the slope factor (19.60). The sensitivity results show that a 25% increase (25% decrease) in the slope factor (19.60) led to a 9.19-18.62% increase (12.69-14.32% decrease) in the maximum HONO production rate and a 0-17.64% increase (8.40-14.07% decrease) in the maximum HONO loss rate (Fig.R2) (section 3.2 in the revised version).

(ii) Unexpected high HONO concentrations have been observed in recent years. However, most current air quality models have underestimated HONO observations, particularly in the daytime (Czader et al., 2012; Gonçalves et al., 2012; Li et al., 2011). Although some of modeling studies have improved HONO daytime simulations by incorporating the new HONO formation mechanisms, e.g., HNO_3 surface photolysis (Sarwar et al., 2008), the NO_2 heterogeneous reaction on aerosols and ground surface (Li et al., 2010; Wong et al., 2013) into air quality models, these HONO daytime formation mechanisms are still under discussion (see the responses to question 1B and 1C of Reviewer #2). Different from these modeling studies above, we derived a formula ($P_{unknown} \approx 19.60[NO_2] \cdot J(NO_2)$) based on the observation data from 13 different field campaigns to quantify the unknown daytime HONO source, and then coupled the $P_{unknown}$ into the WRF-Chem model based on our previous studies (Li et al., 2011; An et al., 2013; Tang et al., 2014). We found that the $P_{unknown}$ significantly improved the daytime HONO simulations. We also assessed the impacts of the $P_{unknown}$ on the concentrations and production and loss rates of HONO, OH, HO_2, and organic peroxy radicals (RO_2).

For modeling study, this is a new and simple method to help quantify the daytime HONO source if the detailed formation mechanism of HONO in the daytime is unknown. However, needed are more field and laboratory studies for the detailed formation mechanism of HONO in the future .

(iii) The uncertainty analysis were added in the section 3.2: *"The maximum $P_{unknown}$ uncertainty range of 25% (Table S1), a 25% increase (decrease) in the slope factor (19.60) led to a 9.19−18.62% increase (12.69−14.32% decrease) in the maximum HONO production rate and a 0−17.64% increase (8.40−14.07% decrease) in the maximum HONO loss rate (Fig. S3 in the Supplement)."*

B. How the model itself and these inputs affect the model output?

In general, the main influencing factors for model output are meteorological fields and the emissions inventory.

(i) Comparison of simulated and observed meteorological factors has been made in our previous study (Wang et al., 2014). The RMSE was 2.5°C for air temperature (TA), 16.3% for relative humidity (RH), 2.5 m s^{-1} for wind speed (WS), and 99.3° for wind direction (WD), whereas the IOA was 0.90 for TA, 0.78 for RH, 0.56 for WS, and 0.65 for WD (Table R2). These statistical metrics indicated that the simulations of TA and RH were much better than those of WS and WD. The results were very similar to the studies of Wang et al. (2010) and Li et al. (2012) using the fifth-generation Pennsylvania State University/National Center for Atmospheric Research Mesoscale Model (MM5), and those of H. Zhang et al. (2012) using the WRF model (Table R2). The definitions of root-mean-square error (RMSE), mean bias (MB), normalized mean bias (NMB), correlation coefficient (RC), and index of agreement (IOA) are available in Simon et al. (2012).

(ii) As for the emissions inventory, monthly anthropogenic emissions of SO_2, NO_x, CO, VOCs, PM_{10}, $PM_{2.5}$, BC, and OC in 2006/2007 were obtained from Zhang et al. (2009) and those of NH_3 from Streets et al. (2003) and monthly emissions of other species were derived from Zhang et al. (2009). The anthropogenic and biogenic emissions were the same as those used by An et al. (2011, 2013), Li et al. (2011, 2014), Tang et al. (2014), and Wang et al. (2014).

(iii) The uncertainty of anthropogenic VOCs (AVOCs) emissions in China is large (Wang et al., 2014). Wang et al. (2014) demonstrated that AVOCs emissions in 2006 from Zhang et al. (2009) were underestimated by ~68% in suburban areas and by more than 68% in urban areas. The substantial underestimation of AVOCs emissions is one of the main reasons for low simulations of HO_2 and low contributions of HO_2+NO in this study. This will be improved in our future work.

C. The model-observation difference is quite considerable in Fig. 4-6. How to make sure your results is a trustful one?

(i) The model performance for O_3 and NO_x in Beijing was good and comparable with other applications of the CMAQ model by Li et al. (2012). However, the model performance in Guangzhou of the PRD region was not as good as that in Beijing. The model-observation

difference in Guangzhou is mainly caused by the underestimation of the emissions inventory. If the emissions are improved, the WRF-Chem model will well simulate the mixing ratios of considered chemical species. Take Beijing as an example, we added the comparison of simulated and observed O_3 at six sites in the BTH (Fig. R3), with an RC of 0.84, NMB of -4.0%, NME of 35.0%, and IOA of 0.91 , better than the results of Li et al. (2012) and Wang et al. (2010).

(ii) Although there are some differences in HONO simulations, we have significantly improved the HONO simulations in both daytime and nighttime.

(iii) The model performance for OH in Guangzhou was good; whereas, that for HO_2 was underestimated. This underestimation was mainly associated with the underestimation of the AVOCs emissions (Wang et al., 2014).

3. In page 809, line 15-17: other OH primary sources, such as HCHO photolysis, is widely accepted. Add them!

According to the previous studies (Alicke et al., 2003; Ren et al., 2003; Lu et al., 2012), the HCHO photolysis is not the direct source of OH. The reaction product of HCHO photolysis is HO_2, which contributes to the OH formation via the reaction of HO_2 with NO. The photochemistry of HCHO is below (Meller and Moortgart, 2000),

$$HCHO + h\nu \rightarrow H + HCO \quad (1)$$

$$HCHO + h\nu \rightarrow H_2 + CO \quad (2)$$

$$H + O_2 \rightarrow HO_2 \quad (3)$$

$$HCO + O_2 \rightarrow HO_2 + CO \quad (4)$$

$$HO_2 + NO \rightarrow OH + NO_2 \quad (5)$$

So we have added "the HO_2 to OH conversion process (HO_2+NO)" in the Introduction section: "*OH is formed primarily through the photolysis of O_3, nitrous acid (HONO), hydrogen peroxide (H_2O_2), the reactions of O_3 with alkenes, and the HO_2 to OH conversion process (HO_2+NO) (Platt et al., 1980; Crutzen and Zimmermann,1991; Atkinson and Aschmann, 1993; Fried et al., 1997; Paulson et al., 1997).***"**

4. In page 809, line 27: if daytime HONO could reach ppb level, it is within the detect limit of most HONO measurement instruments. Do you mean specific instrument here?

According to your suggestions, we have revised them in the Introduction section: "*After sunrise, HONO mixing ratios are usually in low concentrations due to the strong photolysis of*

HONO."

5. In page 813, line 10-14: ambient HONO is correlated with NO_2 as a result of secondary HONO formation instead of HONO direct emission since HONO photolysis lifetime is only about 15 min in the noontime. So why the correlation is the reason for that HONO/NO_x ratio is used as a HONO emission factor?

According to your suggestions, we have revised them in the Introduction section: "*This is the reason why the recent CalNex 2010 (California Research at the Nexus of Air Quality and Climate Change) study found a very strong positive correlation (R^2= 0.985) between HONO flux and the product of NO_2 concentration and solar radiation at Bakersfield site (Ren et al., 2011).***"**

6. In page 814, line 4-7: an annular denuder and an absorption photometer were used for HONO measurement. How are their results comparing to, such as DOAS? How are they compared to each other?

As described in Section 2.1: "*HONO observations were conducted using two annular denuders at the campus of Peking University (PKU) (39°59'N, 116°18'E) in Beijing on 17–20 August 2007 (Spataro et al., 2013) and a long path absorption photometer at the Backgarden (BG) supersite (23°30'N, 113°10'E), about 60 km northwest of Guangzhou on 3–31 July 2006 (X. Li et al., 2012).***"**

(i) HONO can be measured by various techniques, e.g., spectroscopic techniques and wet chemical techniques Differential optical absorption spectroscopy (DOAS) detects HONO by its specific UV absorption ranges with detection limits in the order of 100 ppt (Platt et al., 1980). Wet chemical techniques, which operate HONO sampling on humid/aqueous surfaces, include rotated wet annular denuders and the long path absorption photometer (LOPAP). The techniques have detection limits in the order of few ppt, but suffer from chemical interferences caused by, e.g., NO_2 and phenol reaction or by NO_2 and SO_2 (Gutzwiller et al., 2002; Spindler et al., 2003). However, since the LOPAP instrument collects HONO even at low pH, these chemical interferences are minimized (Kleffmann et al., 2002, 2006). That means the HONO measured by the wet chemical techniques (e.g., annular denuder and LOPAP) could be compared to that by the DOAS.

(ii) Both being the wet chemical techniques, the annular denuder and the LOPAP could be comparable.

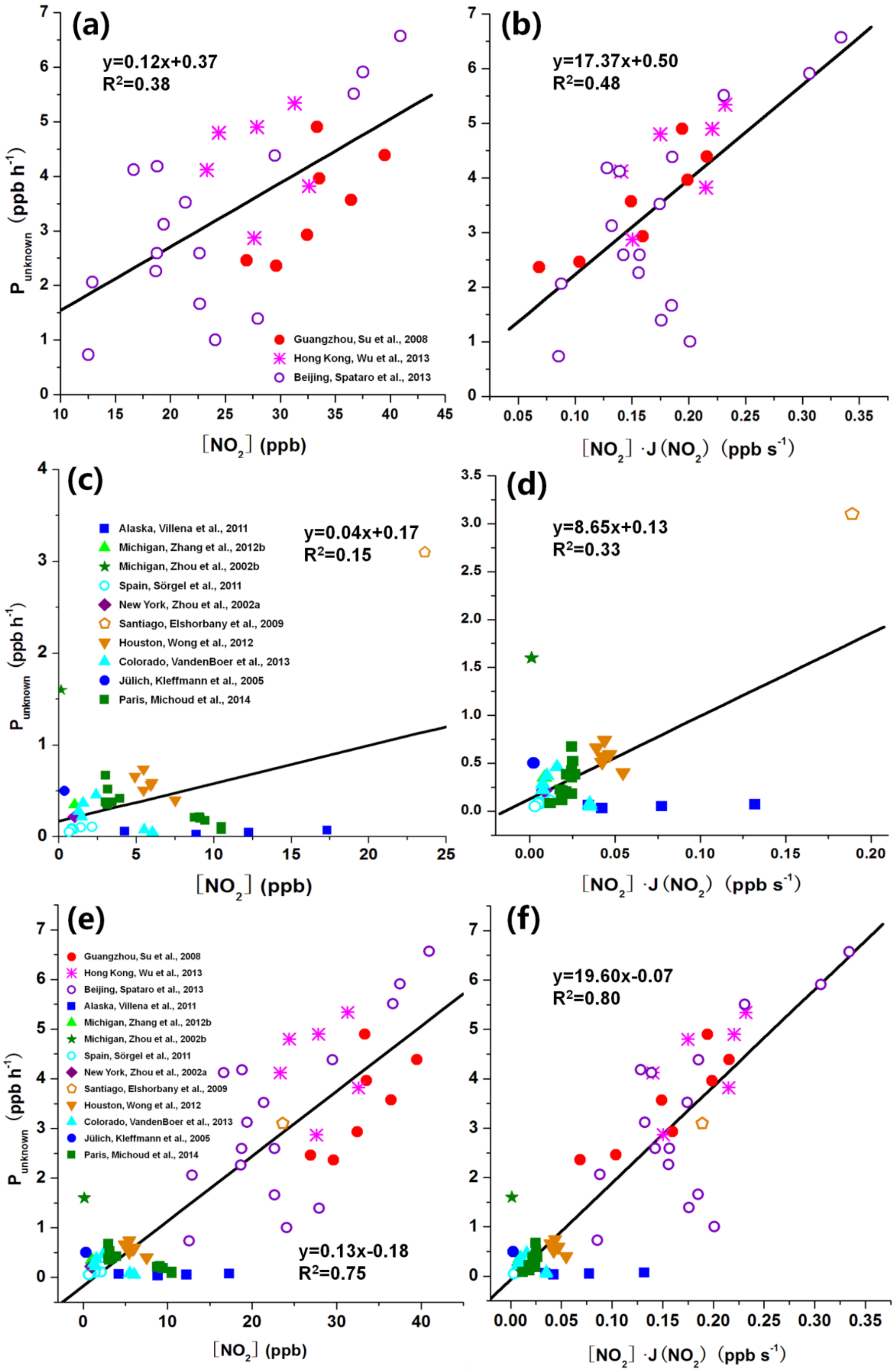

Fig. R1. Correlations of the unknown daytime HONO source ($P_{unknown}$) (ppb h^{-1}) with NO_2 mixing ratios (ppb) and $[NO_2]$ J(NO_2) (ppb s^{-1}) in (a), (b) the coastal regions of China, (c), (d) the other countries, and (e), (f) the globe, respectively, based on the field experiment data shown in Fig. 1 in the revised version.

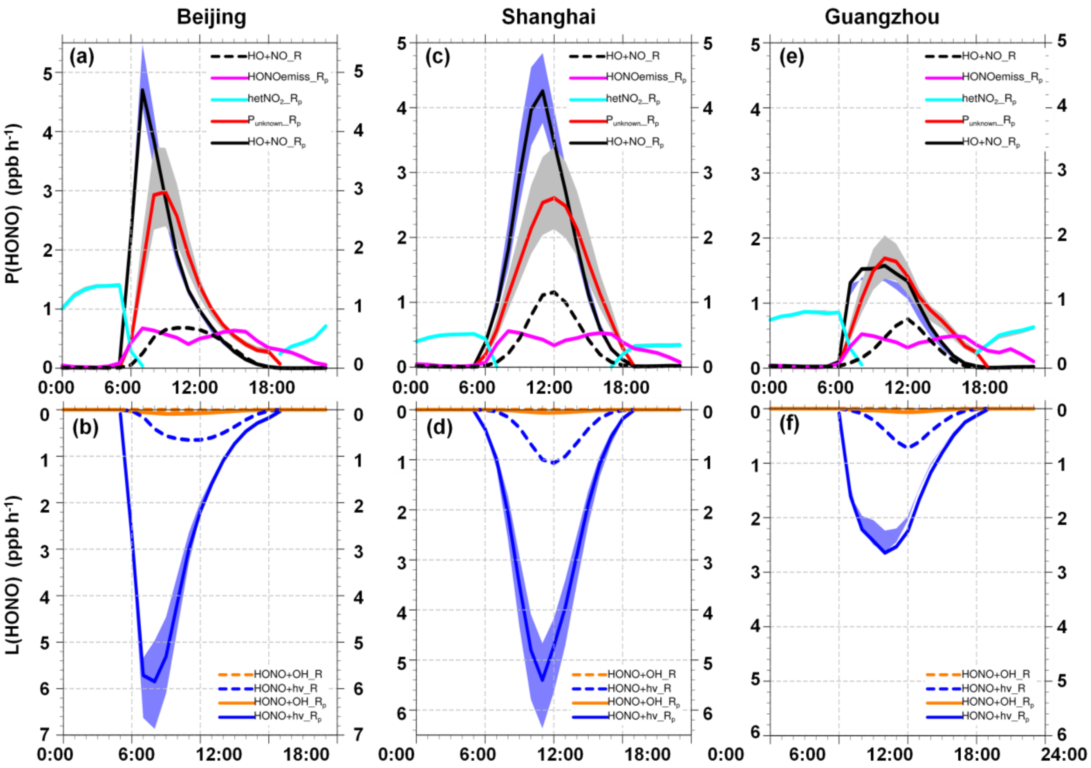

Fig. R2. Production [P(HONO)] and loss [L(HONO)] rates of HONO for cases R (dashed lines), R_p(solid lines) and sensitivity ranges (based on R_{inc} and R_{dec}) in (a), (b) Beijing, (c), (d) Shanghai, and (e), (f) Guangzhou in August 2007. Case R_{inc} includes case R_p with an increase of 25% (the maximum uncertainty range according to the previous studies above) in the slope factor (19.60); Case R_{dec} is the same as case R_p with a decrease of 25% in the slope factor (19.60).

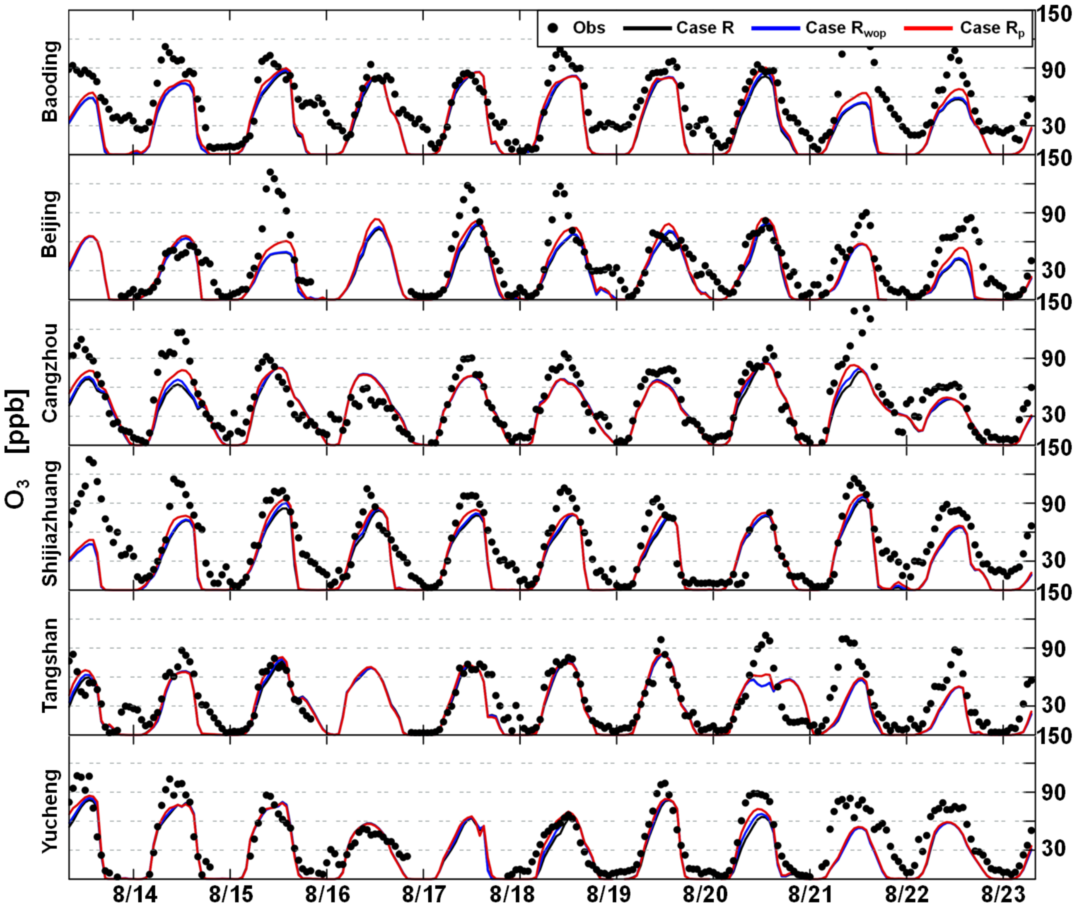

Fig. R3. Comparison of simulated and observed hourly-mean mixing ratios of O_3 (ppb) at six sites in the Beijing-Tianjin-Hebei region (BTH) in August 14-22 of 2007.

Table R1.The calculated unknown daytime HONO source ($P_{unknown}$), NO_2 mixing ratios and photolysis frequency of NO_2 [$J(NO_2)$] from field experiments in Figure 1.

Site	Date	Time	$P_{unknown}$ (ppb h^{-1})	$[NO_2]$ (ppb)	$J(NO_2)$ ($\times 10^{-3}$ s^{-1})	Measurement techniques /Uncertainties	Reference
Xinken (22.6 °N, 113.6 °E)	2004.10.23-2004.10.30	09:30	2.36	29.65	2.31	HONO: WD/IC; NO_2: estimated from NO and NO_y (measured by the NO-O_3 chemiluminescence detector (Kondo et al., 1997))/22%; $J(NO_2)$: TUV/18%; $P_{unknown}$: 10~30%.	Su et al. (2008) Su et al. (2011)
		10:30	3.57	36.46	4.09		
		11:30	4.39	39.51	5.46		
		12:30	4.90	33.33	5.83		
		13:30	3.96	33.54	5.93		
		14:30	2.93	32.43	4.92		
		15:30	2.46	26.94	3.85		
Beijing (39.99 °N, 116.30 °E)	2007.08.17	8:00	2.59	22.66	6.29	HONO: Annular denuders; NO_2: means of commercial ECOTECH Ltd. (Australia analyzer)/ 1%; $J(NO_2)$: calculated by J(HONO);	Spataro et al. (2013)
		10:00	1.66	22.67	8.16		
		12:00	1.00	24.09	8.35		
		14:00	3.12	19.39	6.82		
	2007.08.18	8:00	1.39	27.96	6.29		
		10:00	3.52	21.37	8.16		
		12:00	4.12	16.66	8.35		
		14:00	2.06	12.90	6.82		
	2007.08.19	8:00	4.38	29.50	6.29		
		10:00	5.91	37.53	8.16		
		12:00	2.26	18.67	8.35		
		14:00	0.73	12.54	6.82		
	2007.08.20	8:00	5.51	36.69	6.29		
		10:00	6.57	40.94	8.16		

		12:00	2.59	18.78	8.35		
		14:00	4.18	18.79	6.82		
Tung Chung (22.30 °N, 113.93 °E)	2011.08.25-2011.08.31	10:00	2.87	27.62	5.45	HONO: LOPAP; NO_2: TEI; J(NO_2): Optical actinometer.	Wu et al. (2013)
		11:00	3.82	32.62	6.59		
		12:00	5.34	31.31	7.41		
		13:00	4.90	27.86	7.92		
		14:00	4.80	24.40	7.17		
		15:00	4.12	23.33	6.02		
Alaska (71.32 °N, 156.65 °W)	2009.03.13-2009.04.14	10:30	0.03	-	4.73	HONO: LOPAP; NO_2: estimated from NO and NO_y (measured by the NO-O_3 chemiluminescence detector; J(NO_2): estimated as a function of solar zenith angle using the TUV radiative transfer model.	Villena et al. (2011)
		11:00	0.03	-	6.03		
		11:30	0.06	4.23	8.16		
		12:00	0.09	-	8.81		
		12:30	0.05	-	9.46		
		13:00	0.08	-	8.69		
		13:30	0.07	17.31	7.63		
		14:00	0.05	12.24	6.33		
		14:30	0.03	8.85	4.79		
Michigan (45.50 °N, 84.70 °W)	2008.07.17-2008.08.07	noon	0.35	1.00	8.48	HONO: LOPAP; NO_2: Custom-built analyzer using the chemiluminescence technique; J(NO_2): estimated as a function of UV measured by the TUV radiative transfer model/10%.	N. Zhang et al. (2012)
Michigan (45.50 °N, 84.70 °W)	2000.07.27	noon	1.60	0.13	8.48	HONO: Two-channel measurement system (Zhou et al., 1999); NO_2: TEI Model.	Zhou et al. (2002a)

Spain (37.10 °N, 6.74 °W)	2008.07.17- 2008.08.07 (cloud-free)	10:00	0.11	2.15	5.39	HONO: LOPAP/12%; NO_2: Droplet Measurement Technologies (Hosaynali-Beygi et al., 2011) /8%; $J(NO_2)$: Filter radiometers/5%; $P_{unknown}$: 18%.	Sörgel et al. (2011)
		11:00	0.10	1.38	6.26		
		12:00	0.08	0.95	6.76		
		13:00	0.09	0.84	6.68		
		14:00	0.08	0.79	6.03		
		15:00	0.05	0.66	4.62		
New York (42.09 °N, 77.21 °W)	1998.06.26- 1998.07.14	noon	0.22	1.00	8.48	HONO: Two-channel measurement system (Zhou et al., 1999); NO_2: TEI Model.	Zhou et al. (2002b)
Santiago (33.45 °S, 70.67 °W)	2005.03.08- 2005.03.20	noon	1.70	10.00	8.00	HONO: LOPAP; NO_2: DOAS-OPSIS optical system; $J(NO_2)$: Filter radiometers.	Elshorbany et al. (2009)
Houston (29.76 °N, 95.37 °W)	2009.04.21	10:00	0.40	7.50	7.29	HONO: LP-DOAS/5%; NO_2: LP-DOAS /3%; $J(NO_2)$: SAFS; $P_{unknown}$: 10~20%.	Wong et al. (2012)
		11:00	0.59	6.02	7.77		
		12:00	0.74	5.45	8.03		
		13:00	0.66	4.89	8.03		
		14:00	0.51	5.45	7.76		
		15:00	0.57	5.91	7.18		
Colorado (40.05 °N, 105.00 °W)	2011.02.19- 2011.02.25	10:00	0.05	6.04	5.84	HONO: NI-PT-CIMS; NO_2: a cavity ring-down spectrometer (Wagner et al., 2011)/5%; $J(NO_2)$: Filter radiometers.	VandenBoer et al. (2013)
		11:00	0.08	5.49	6.39		
		12:00	0.46	2.39	6.64		
		13:00	0.37	1.55	6.39		
		14:00	0.28	1.27	6.02		
		15:00	0.22	1.47	5.22		
Jülich	2003.07.29	noon	0.50	0.35	6.63	HONO: LOPAP;	Kleffmann et al. (2005)

(50.92 °N, 6.36 °E)						NO_2: Chemiluminescence analyzer equipped with a photolytic converter for NO_2 to NO conversion; J(NO_2): derived from actinic flux spectra measured by a scanning spectroradiometer.	
Paris (40.72 °N, 2.21 °E)	2009.07.09-2009.07.27	10:00	0.42	3.91	6.31	HONO: Wet chemical derivatization (SA/NED), HPLC detection (NitroMAC)/12%; NO_2: Luminol chemiluminescence/5%; J(NO_2): filter radiometer/ 20–25%.	Michoud et al. (2014)
		11:00	0.38	3.42	7.76		
		12:00	0.52	3.14	8.08		
		13:00	0.67	3.00	8.24		
		14;00	0.38	3.00	7.29		
		15:00	0.35	3.11	7.88		
	2010.01.15-2010.02.15	10:00	0.08	10.49	1.16		
		11:00	0.11	10.49	1.80		
		12:00	0.18	9.44	2.60		
		13:00	0.21	8.76	2.20		
		14;00	0.20	9.12	2.34		
		15:00	0.22	9.07	1.99		

WD/IC: Wet Denuder sampling/Ion Chromatograph analysis system; TUV: Ultraviolet-Visible Model; TEI: Thermo Environmental Instruments; LOPAP: Long path absorption photometer; LP-DOAS: Long path Differential Optical Absorption Spectroscopy instrument; SAFS: scanning actinic flux spectroradiometer; NI-PT-CIMS: Negative-Ion Proton-Transfer Mass Spectrometer; SA/NED: an aqueous sulphanilamide/ N-(1-naphthyl)-ethylenediamine solution; NitroMAC: an instrument developed at the laboratory (Afif et al., 2014); HPLC: High Performance Liquid Chromatography.

Note that: Since J(NO_2) data of Wu et al. (2012), N. Zhang et al. (2012), Zhou et al. (2002b), VandenBoer et al. (2013), Kleffmann et al. (2005) were not measured, they were calculated from the J(HONO) measurement data (J(NO_2) = 5.3J(HONO)) (Kraus and Hofzumahaus, 1998); J(NO_2) data of Zhou et al. (2002ab) were derived from the campaign of N. Zhang et al. (2012) (The experiments were conducted in summer and the studied sites were close to each other). J(NO2) data of Spataro et al. (2013) were also calculated from the J(HONO) at noon (J(NO_2) = 5.3J(HONO)), then we computed the hourly J(NO_2) (8:00~14:00 LST) through multiplying by the cosine of solar zenith angle. The NO_2 mixing ratios of N. Zhang et al. (2012) and Zhou et al. (2002b) were not shown and derived from NO_x mixing ratios. Similarly, NO_2 mixing ratios of Kleffmann et al. (2005) were inferred from NO mixing ratios.

Table R2. Performance metrics of WRF-Chem meteorology simulations in August 2007 (Wang et al., 2014)

Temperature(℃)			Relative Humidity(%)			Wind Speed(m/s)			Wind direction(deg)			Reference
RMSE	MB	IOA	RMSE	MB	IOA	RMSE	MB	IOA	RMSE	MB	IOA	
2.54	0.23	0.90	16.30	-5.46	0.78	2.46	1.61	0.56	99.25	2.59	0.65	This work
	-0.88	0.90		-1.30	0.78	2.06	0.89	0.65		2.47		(Wang et al., 2010b)
	0.53	0.88		-1.06	0.86	1.47	0.64	0.62		2.59		(Li et al., 2012)
3.1	0.8		17.4	-5.7		2.2	1.1		60.9	8.2		(H. Zhang et al., 2012)

References

Afif, C., Jambert, C., Colomb, A., Eyglunent, G., Borbon, A., Daële, V., Doussin, J. F., and Perros, P. E.: NitroMAC: an instrument for the measurement of HONO. Intercomparison with LOPAP, Water Air Soil Poll., in preparation, 2014.

An, J., Zhang, W., Qu Y.: Impacts of a strong cold front on concentrations of HONO, HCHO, O_3, and NO_2 in the heavy traffic urban area of Beijing, Atmospheric Environment, 43, 3454–3459, 2009.

An, J., Li, Y., Wang, F., and Xie, P.: Impacts of photoexcited NO_2 chemistry and heterogeneous reactions on concentrations of O_3 and NO_y in Beijing, Tianjin and Hebei province of China, Air Quality-Models and Applications, Prof. Dragana Popovic (Ed.), InTech, ISBN: 978-953-307-307-1, doi: 10.5772/16858, 2011.

An, J., Li, Y., Chen, Y., Li, J., Qu, Y., Tang, Y.: Enhancements of major aerosol components due to additional HONO sources in the North China Plain and implications for visibility and haze, Advances in Atmospheric Science, 30, 57-66, 2013.

Alicke, B., Geyer, A., Hofzumahaus, A., Holland, F., Konrad, S., Pätz, H. W., Schäfer, J., Stutz, J., Volz-Thomas, A., Platt, U.: OH formation by HONO photolysis during the BERLIOZ experiment, Journal of Geophysical Research, 108, D4, 8247, doi:10.1029/2001JD000579, 2003.

Czader, B. H., Rappenglück, B., Percell, P., Byun, D. W., Ngan, F., and Kim, S.: Modeling nitrous acid and its impact on ozone and hydroxyl radical during the Texas Air Quality Study 2006, Atmos. Chem. Phys., 12, 6939–6951, doi:10.5194/acp-12-6939-2012, 2012.

Elshorbany, Y. F., Kurtenbach, R., Wiesen, P., Lissi, E., Rubio, M., Villena, G., Gramsch, E., Rickard, A. R., Pilling, M. J., Kleffmann, J.: Oxidation capacity of the city air of Santiago, Chile. Atmospheric Chemistry and Physics, 9(6), 2257-2273, 2009.

Gonçalves, M., Dabdub, D., Chang, W. L., Jorba, O., and Baldasano, J. M.: Impact of HONO sources on the performance of mesoscale air quality models, Atmos. Environ., 54, 168–176, 2012.

Gutzwiller L, Arens F, Baltensperger U, Gäggeler HW, Ammann M. Significance of semivolatile diesel exhaust organics for secondary HONO formation, Environ Sci Technol, 36, 677-682, 2002.

Hosaynali Beygi, Z., Fischer, H., Harder, H. D., Martinez, M., Sander, R., Williams, J., Brookes, D. M., Monks, P. S., and Lelieveld, J.: Oxidation photochemistry in the Southern Atlantic boundary layer: unexpected deviations of photochemical steady state, Atmos. Chem. Phys., 11, 8497–8513, doi:10.5194/acp-11-8497-2011, 2011.

Kleffmann, J., Heland, J., Kurtenbach, R., Lörzer, J., Wiesen, P.: A new instrument for the detection of nitrous acid (HONO), Environ Sci Pollut Res, 4(Special Issue 4), 48–54. 2002.

Kleffmann, J., Gavriloaiei, T., Hofzumahaus, A., Holland, F., Koppmann, R., Rupp, L.,Schlosser, E., Siese, M., and Wahner, A.: Daytime formation of nitrous acid: a major source of OH radicals in a forest, J. Geophys. Res. Lett., 32(5), doi: 10.1029/2005GL022524, 2005.

Kleffmann, J., Lorzer, J. C., Wiesen, P., Kern, C., Trick, S., Volkamer, R.: Intercomparison of the DOAS and LOPAP techniques for the detection of nitrous acid (HONO), Atmos Environ, 40, 3640-3652, 2006.

Kondo, Y., S. Kawakami, M. Koike, D. Fahey, H. Nakajima, Y. Zhao, N. Toriyama, M. Kanada, G. Sachse, and G. Gregory.: The performance of an aircraft instrument for the measurement of NO_y. J. Geophys. Res., 102, 28,663–28,671, 1997.

Li, G., Lei, W., Zavala, M., Volkamer, R., Dusanter, S., Stevens, P., Molina, L.T.: Impacts of HONO sources on the photochemistry in Mexico City during the MCMA-2006/MILAGO Campaign, Atmos. Chem. Phys. 10, 6551-6567, 2010.

Li, L., Chen, C. H., Huang, C., Huang, H. Y., Zhang, G. F., Wang, Y. J., Wang, H. L., Lou, S. R., Qiao, L. P., Zhou, M., Chen, M. H., Chen, Y. R., Fu, J. S., Streets, D. G., Jang, C. J.: Process analysis of regional ozone formation over the Yangtze River Delta, China using the Community Multi-scale Air Quality modeling system, Atmospheric Chemistry and Physics, 12, 10971-10987, 2012.

Li, Y., An, J., Min, M., Zhang, W., Wang, F., Xie, P.: Impacts of HONO sources on the air quality in Beijing, Tianjin and Hebei Province of China, Atmospheric Environment, 45(27), 4735-4744, 2011.

Li, Y., An, J., Gultepe I.: Effects of additional HONO sources on visibility over the North China Plain, Adv. Atmos. Sci., 31(5), 1221–1232, doi: 10.1007/s00376-014-4019-1, 2014.

Lu, K. D., Rohrer, F., Holland, F., Fuchs, H., Bohn, B., Brauers, T., Chang, C. C., Haseler, R., Hu, M., Kita, K., Kondo, Y., Li, X., Lou, S. R., Nehr, S., Shao, M., Zeng, L. M., Wahner, A., Zhang, Y. H., Hofzumahaus, A.: Observation and modelling of OH and HO_2 concentrations in the Pearl River Delta 2006: a missing OH source in a VOC rich atmosphere, Atmospheric Chemistry and Physics, 12(3), 1541-1569, 2012.

Meller, R. and Moortgat, G. K.: Temperature dependence of the absorption cross sections of formaldehyde between 223 and 323 k in the wavelength range 225–375 nm, J. Geophys. Res.-Atmos., 105, 7089–7101, 2000.

Michoud, V., Colomb, A., Borbon, A., Miet, K., Beekmann, M., Camredon, M., Aumont, B., Perrier, S., Zapf, P., Siour, G., Ait-Helal, W., Afif, C., Kukui, A., Furger, M., Dupont, J. C., Haeffelin, M., Doussin, J. F.: Study of the unknown HONO daytime source at a European suburban site during the MEGAPOLI summer and winter field campaigns. Atmospheric Chemistry and Physics, 14(6), 2805-2822, 2014.

Platt, U., Perner, D., Harris, G. W., Winer, A. M., Pitts, J. N.: Observations of nitrous acid in an urban atmosphere by differential optical absorption, Nature 285, 312-314 (29 May 1980); doi: 10.1038/285312a0, 1980.

Ren, X., Harder, H., Martinez, M., Lesher, R. L., Oliger, A., Simpas, J. B., Brunea, W. H., Schwab, J. J., Demerjian, K. L., He, Y., Zhou, X., Gao, H.: OH and HO_2 Chemistry in the urban atmosphere of New York City, Atmospheric Environment, 37(26), 3639-3651, 2003.

Rohrer, F., Bohn, B., Brauers, T., Brüning, D., Johnen, F. J., Wahner, A., Kleffmann, J.: Characterisation of the photolytic HONO-source in the atmosphere simulation chamber SAPHIR, Atmospheric Chemistry and Physics, 5(8), 2189-2201, 2005.

Sörgel, M., Regelin, E., Bozem, H., Diesch, J. M., Drewnick, F., Fischer, H., Harder, H., Held, A., Hosaynali-Beygi, Z., Martinez, M., Zetzsch, C.: Quantification of the unknown HONO daytime source and its relation to NO_2, Atmospheric Chemistry and Physics, 11(20), 10433-10447, 2011.

Sarwar, G., Roselle, S. J., Mathur, R., Appel, W., Dennis, R. L., Vogel, B.: A comparison of CMAQ HONO predictions with observations from the Northeast Oxidant and Particle Study, Atmospheric Environment, 42(23), 5760-5770, 2008.

Spataro, F., Ianniello, A., Esposito, G., Allegrini, I., Zhu, T., Hu, M.: Occurrence of atmospheric nitrous acid in the urban area of Beijing (China), Science of the Total Environment, 447, 210-224, 2013.

Simon, H., Baker, K. R., Phillips, S.: Compilation and interpretation of photochemical model performance statistics published between 2006 and 2012, Atmos. Environ., 61, 124-139, 2012.

Spindler, G., Hesper, J., Brüggemann, E., Dubois, R., Müller, Th., Herrmann, H.: Wet annular denuder measurements of nitrous acid: laboratory study of the artifact reaction of NO2 with S(IV) in aqueous solutions and comparison with field measurements, Atmos Environ, 37, 2643-2662, 2003.

Streets, D. G., Bond, T. C., Carmichael, G. R., Fernandes, S. D., Fu, Q., He, D., Klimont, Z., Nelson, S. M., Tsai, N. Y., Wang, M. Q., Woo, J. H., Yarber, K. F.: An inventory of gaseous and primary aerosol emissions in Asia in the year 2000, Journal of Geophysical Research, Atmospheres 108, 8809, 2003.

Su, H., Cheng, Y., Oswald, R., Behrendt, T., Trebs, I., Meixner, F. X., Andreae, M. O., Cheng, P., Zhang, Y., Pöschl, U.: Soil nitrite as a source of atmospheric HONO and OH radicals, Science, 333(6049), 1616-1618, 2011.

Su, H., Cheng, Y. F., Shao, M., Gao, D. F., Yu, Z. Y., Zeng, L. M., Slanina, J., Zhang, Y. H., Wiedensohler, A.: Nitrous acid (HONO) and its daytime sources at a rural site during the 2004 PRIDE‐PRD experiment in China, Journal of Geophysical Research: Atmospheres (1984–2012), 113(D14), 2008.

Tang, Y., An, J., Li, Y., Wang, F.: Uncertainty in the uptake coefficient for HONO formation on soot and its impacts on concentrations of major chemical components in the Beijing–Tianjin–Hebei region, Atmospheric Environment, 84, 163-171, 2014.

VandenBoer, T. C., Brown, S. S., Murphy, J. G., Keene, W. C., Young, C. J., Pszenny, A. A. P., Kim, S., Warneke, C., de Gouw, J. A., Maben, J. R., Wagner, N. L., Riedel, T. P., Thornton, J. A., Wolfe, D. E., Dubé, W. P., Öztürk, F., Brock, C. A., Grossberg, N., Lefer, B., Lerner, B. Middlebrook, A. M., Roberts, J. M.: Understanding the role of the ground surface in HONO vertical structure: High resolution vertical profiles during NACHTT-11. Journal of Geophysical Research: Atmospheres, 118, 10,155–10,171, doi:10.1002/jgrd.50721, 2013.

Villena, G., Wiesen, P., Cantrell, C. A., Flocke, F., Fried, A., Hall, S. R., Hornbrook, R. S., Knapp, D., Kosciuch, E., Mauldin, R. L., McGrath, J. A., Montzka, D., Richter, D., Ullmann, K., Walega, J., Weibring, P., Weinheimer, A., Staebler, R. M., Liao, J., Huey, L. G., and Kleffmann, J.: Nitrous acid (HONO) during polar spring in Barrow, Alaska: a net source of OH radicals?, J. Geophys. Res. –Atmos., 116(D14), doi: 10.1029/2011JD016643, 2011.

Wagner, N. L., Dubé, W. P., Washenfelder, R. A., Young, C. J., Pollack, I. B., Ryerson, T. B., Brown S. S.: Diode laser-based cavity ring-down instrument for NO_3, N_2O_5, NO, NO_2 and O_3 from aircraft, Atmos. Meas. Technol., 4, 1227–1240, 2011.

Wang, F., An, J., Li, Y., Tang, Y., Lin, J., Qu, Y., Cheng, Y., Zhang, B., Zhai, J.: Impacts of Uncertainty in AVOC Emissions on the Summer RO_x Budget and Ozone Production Rate in the Three Most Rapidly-Developing Economic Growth Regions of China, Advances in Atmospheric Sciences, 31, 1331–1342, 2014.

Wang, X., Zhang, Y., Hu, Y., Zhou, W., Lu, K., Zhong, L., Zeng, L., Shao, M., Hu, M., Russell, A. G.: Process analysis and sensitivity study of regional ozone formation over the Pearl River Delta, China, during the PRIDE-PRD2004 campaign using the Community Multiscale Air Quality modeling system, Atmospheric Chemistry and Physics, 10(9), 4423-4437, 2010.

Wong, K. W., Tsai, C., Lefer, B., Haman, C., Grossberg, N., Brune, W. H., Ren, X., Luke, W., Stutz, J.: Daytime HONO vertical gradients during SHARP 2009 in Houston, TX, Atmospheric Chemistry and Physics, 12(2), 635-652, 2012.

Wong, K. W., Tsai, C., Lefer, B., Grossberg, N., Stutz, J.: Modeling of daytime HONO vertical gradients during SHARP 2009, Atmospheric Chemistry and Physics, 13(7), 3587-3601, 2013.

Wu, J., Xu, Z., Xue, L., and Wang, T.: Daytime nitrous acid at a polluted suburban site in Hong Kong: indication of heterogeneous production on aerosol, in: Proceedings of 12th international conference on atmospheric sciences and applications to air quality, Seoul, Korea, 3–5 June 2013, 52, 2013.

Zhang, Q., Streets, D. G., Carmichael, G. R., He, K., Huo, H., Kannari, A., Klimont, Z., Park, I., Reddy, S., Fu, J. S., Chen, D., Duan, L., Lei, Y., Wang, L., Yao, Z.: Asian emissions in 2006 for the NASA INTEX-B mission, Atmospheric Chemistry and Physics, 9, 5131-5153, 2009.

Zhang, H., Li, J., Ying, Q., Yu, J. Z., Wu, D., Cheng, Y., Kebin Hed, Jiang, J.: Source apportionment of $PM_{2.5}$ nitrate and sulfate in China using a source-oriented chemical transport model. Atmospheric Environment, 62, 228-242, 2012.

Zhang, N., Zhou, X., Bertman, S., Tang, D., Alaghmand, M., Shepson, P. B., Carroll, M. A.: Measurements of ambient HONO concentrations and vertical HONO flux above a northern Michigan forest canopy. Atmospheric Chemistry and Physics, 12(17), 8285-8296, 2012.

Zhou, X., Qiao, H., Deng, G., Civerolo, K.: A method for the measurement of atmospheric HONO based on DNPH derivatization and HPLC analysis. Environ. Sci. Technol., 33, 3672–3679, 1999

Zhou, X., Civerolo, K., Dai, H., Huang, G., Schwab, J., Demerjian, K. Summertime nitrous acid chemistry in the atmospheric boundary layer at a rural site in New York State, Journal of Geophysical Research: Atmospheres (1984–2012), 107(D21), ACH-13, 2002a.

Zhou, X., He, Y., Huang, G., Thornberry, T. D., Carroll, M. A., and Bertman, S. B.: Photochemical production of nitrous acid on glass sample manifold surface, Geophys. Res. Lett., 29, 26-1 – 26-4, doi: 10.1029/2002GL015080, 2002b.

Zhou, X., Gao, H., He, Y., Huang, G., Bertman, S. B., Civerolo, K., Schwab, J.: Nitric acid photolysis on surfaces in low−NO_x environments.: Significant atmospheric implications, Geophysical Research Letters, 30(23), 2003.

Ziemba, L. D., Dibb, J. E., Griffin, R. J., Anderson, C. H., Whitlow, S. I., Lefer, B. L., Rappenglück, B., Flynn, J.: Heterogeneous conversion of nitric acid to nitrous acid on the surface of primary organic aerosol in an urban atmosphere, Atmos. Environ. 44, 4081-4089, 2010